DETAILS ON METHODS

Sampling design. 466 dead specimens of the deposit feeder *Nuculana taphria* and the mixed deposit-feeder/chemosymbiontic *Parvilucina tenuisculpta* were sampled in sediment collected with Van Veen grabs during the Southern California Bight 2003 Regional Monitoring Program (Ranasinghe et al. 2007) (Figure DR1; Table DR1). In grabs yielding >25 specimens of a species, we assigned a unique number to each specimen and then randomly selected 25 specimens per species per grab. Six empty shells of *Nuculana taphria* from two shelf sites at 89 m (Stebbins et al. 2004) were used to calibrate the rate of AAR using ^{14}C dating (Table DR2). We pooled the sites into regional single-species assemblages corresponding to 4 continental shelf segments (Fig. DR1). *Parvilucina* populations were high in the early 1970s on the Palos Verdes shelf but quickly declined in the mid-1980s (LACSD 2012).

Details on shell storage, screening, and AAR procedure. All empty shells plus one live-collected specimen of *Parvilucina tenuisculpta* and one live-collected specimen of *Nuculana elenensis* (a congener of *N. taphria*) had been stored in ethanol for 2 years, after initial exposure of ~2 days to buffered formalin (Ranasinghe et al. 2007). After decanting the ethanol, the shells were air-dried and stored at the University of Chicago. The live-collected specimens were articulated, with (dried) soft-tissue inside, and received the same treatment as the empty shells.

Shells were analyzed for amino acid racemization (AAR) at Northern Arizona University following Kaufman and Manley (1998). Each valve was split in two, and anterior portions of valves, whenever possible (some valves were too small), were analyzed. The posterior portions of a subset of specimens were used for AMS ^{14}C dating. Specimens were sonicated for ~ 4 minutes, leached 20-30% by weight with a 2M solution of HCl. Four screening procedures (Kosnik and Kaufman, 2008) were used to detect aberrant specimens, defined as lying outside the 0.997 quantile (Fig. DR2). Specimens were tested for strength of correlation between (1) serine concentrations (standardized by the concentration of glutamic acid) and aspartic acid D/L^{e}, (2) serine concentration (standardized by the concentration of aspartic acid) and glutamic acid D/L^{e}, (3) total concentrations of aspartic acid and glutamic acid, and (4) aspartic acid D/L^{e} and glutamic acid D/L. Six shells were flagged as outliers, but on <3 methods, thus all were used.

Radiocarbon ages for calibration of AAR ratios. Following standard procedures, 8 specimens of *Parvilucina tenuisculpta* and 11 of *Nuculana taphria* were selected for AMS ^{14}C dating at the NOSAMS facility, Woods Hole (Table DR2). To avoid contamination, ~30% of the outer shell mass was removed prior to analysis. Two *Parvilucina* and 1 *Nuculana* yielded post-bomb ^{14}C ages. Radiocarbon ages were converted to calendar years using Calib6.0 (Stuiver and Reimer 1993), using the Marine04 data (Hughen et al. 2004). A regional marine reservoir correction (ΔR) was determined to be 234 years (standard deviation = 96) on the basis of the ^{14}C age of 12 samples from southern California in the Marine Reservoir Correction Database (calib.qub.ac.uk/marine). The calendar age corresponds to the median of the age probability function, and the uncertainty to the 2σ age range. Calib6.0 does not calibrate marine samples when conventional age minus ΔR is less than 460 ^{14}C yr BP. All ages are calibrated relative to

AD 2003, the year of collection. The analytical error expressed by two standard deviations spans from 171 to 553 years (mean = 293 years, standard deviation = 113 years).

To estimate ages from AAR, the D/L values were raised to a power-law exponent e estimated with numerical optimization that simultaneously minimized (1) differences between the measured ^{14}C age and age predicted by the linear relationship between D/L^e and the calibrated ^{14}C age, divided by the measured ^{14}C age, and (2) differences between age estimates derived from aspartic and glutamic acid, divided by the measured ^{14}C age (Fig. DR2-4, Table DR3). By minimizing proportional residuals, the calibrations equally minimize the regression errors associated with young and old ages. The calibration curves were constrained to pass through the origin. The D/L of live-collected specimens was used as the D/L value for zero age. The shell ages are computed as $b*([D/L]^e – [D/L]_{alive}^e)$, where b is a slope, e a power-law exponent. The mean calibrated AAR age (averaged over the amino acids), weighted by the inverse of the standard error of the age squared, and the error in the weighted mean are computed according to Bevington and Robinson (1992, equations 4.17 and 4.19; Kosnik et al. 2013).

Statistical analyses. When predicting the median and range under a combination of model parameters, we truncate the distributions at 25,000 years, a liberal estimate for the last glacial maximum, and a possible age of some shells at the shelf-slope break, if the break was not fully exposed at lowstand. We calculate confidence intervals on median and range using a bootstrapping approach with 5,000 iterations, following Kowalewski et al. (1998; Krause et al. 2010).

References
Bemis, B.E., Spero, H.J., and Thunell, R.C., 2002, Using species-specific paleotemperature equations with foraminifera: a case study in the Southern California Bight. Marine Micropaleontology, v. 46, p. 405-430.
Bergen, M., Weisberg, S.B., Cadien, D., Dalkey, A., Montagne, D., Smith, R.W., Stull, J.K., and Velarde, R.G., 1998, Southern California Bight 1994 Pilot Project: IV. Benthic Infauna. Southern California Coastal Water Research Project, Westminster, CA., 260 p.
Bevington, P.R., and Robinson, D.K., 1992, Data reduction and error analysis for the physical sciences. Third edition, McGraw Hill, Boston.
Hughen, K.A., Baillie, M.G.L., Bard, E., Bayliss, A., Beck, J.W., Bertrand, C.J.H., Blackwell, P.G., Buck, C.E., Burr, G.S., Cutler, K.B., Damon, P.E., Edwards, R.L., Fairbanks, R.G., Friedrich, M., Guilderson, T.P., Kromer, B., McCormac, F.G., Manning, S.W., Bronk Ramsey, C., Reimer, P.J., Reimer, R.W., Remmele, S., Southon, J.R., Stuiver, M., Talamo, S., Taylor, F.W., van der Plicht, J., and Weyhenmeyer, C.E., 2004, Marine04 Marine radiocarbon age calibration, 26 - 0 ka BP: Radiocarbon, v. 46, p. 1059-1086.
Kaufman, D.S., and Manley, W.F., 1998, A new procedure for determining DL amino acid ratios in fossils using reverse phase liquid chromatography: Quaternary Science Reviews, v. 17, p. 987–1000.
Kosnik, M.A., and Kaufman, D.S., 2008, Identifying outliers and assessing the accuracy of amino acid racemization measurements for geochronology: II. Data screening: Quaternary Geochronology, v. 3, p. 328-341.

Kosnik, M.A., Kaufman, D.S., and Hua, Q., 2013, Radiocarbon-calibrated multiple amino acid geochronology of Holocene molluscs from Bramble and Rib reefs (Great Barrier Reef): Quaternary Geochronology, v. 16, p. 73-86.

Kowalewski, M., Goodfriend, G.A., and Flessa, K.W., 1998, High resolution estimates of temporal mixing within shell beds: the evils and virtues of time-averaging: Paleobiology, v. 24, p. 287–304.

Krause, R.A., Jr., Barbour, S.L., Kowalewski, M., Kaufman, D.S., Romanek, C.S., Simoes, M.G., and Wehmiller, J.F., 2010, Quantitative estimates and modeling of time averaging in bivalve and brachiopod shell accumulations: Paleobiology, v. 36, p. 428–452.

LACSD (Los Angeles County Sanitation Districts), 2012, Joint Water Pollution Control Plant Biennial Receiving Water Monitoring Report 2010-2011. Whittier, CA: LACSD, Ocean Monitoring and Research Group, Technical Services Department, p. 1-154.

Nardin, T.R., Osborne, R.H., Bottjer, D.J., and Scheidemann, R.C., 1981, Holocene sea-level curves for Santa Monica Shelf, Southern California Borderland. Science, v. 213, p. 331-333.

Ohman, M.D., and Venrick, E.L., 2003, CalCOFI in a Changing Ocean. Oceanography, v. 16, p. 76-85.

Ranasinghe, J.A., Montagne, D.E., Smith, R.W., Mikel, T., Weisberg, S.B., Cadien, D., Velarde, R., and Dalkey, A., 2003, Southern California Bight 1998 Regional Monitoring Program: VII. Benthic Macrofauna. Southern California Coastal Water Research Project, Westminster, CA, p. 1-91.

Ranasinghe, J.A., Barnett, A.M., Schiff, K., Montagne, D.E., Brantley, C., Beegan, C., Cadien, D.B., Cash, C., Deets, G.B., Diener, D.R., Mikel, T.K., Smith, R.W., Velarde, R.G., Watts, S.D., and Weisberg, S.B., 2007, Southern California Bight 2003 Regional Monitoring Program: III. Benthic Macrofauna. Southern California Coastal Water Research Project. Costa Mesa, CA, p. 1-44.

Ranasinghe, J.A., Schiff, K.C., Brantley, C.A., Lovell, L.L., Cadien, D.B., Mikel, T.K., Velarde, R.G., Holt,S., and Johnson, S.C., 2012, Southern California Bight 2008 Regional Monitoring Program: VI. Benthic Macrofauna. Southern California Coastal Water Research Project. Costa Mesa, CA, p. 1-71.

Stebbins, T.D., Schiff, K.C., and Ritter, K., 2004, San Diego Sediment Mapping Study: Workplan for Generating Scientifically Defensible Maps of Sediment Conditions in the San Diego Region. City of San Diego, Metropolitan Wastewater Department, Environmental Monitoring and Technical Services Division, and Southern California Coastal Water Research Project, Westminster, CA, p. 1-11.

Stuiver, M., and Reimer, P.J., 1993, Extended ^{14}C database and revised CALIB 3.0 C age calibration program: Radiocarbon, v. 35, p. 215–230.

Thompson, B., Tsukada, D., and O'Donohue, D., 1993, 1990 Reference Site Survey. Southern California Coastal Water Research Project (SCCWRP), Technical Report #269, p. 1-105. 7171 Fenwick Lane, Westminster, CA 92683.

Codes in the R language for fitting the Weibull and two-phase model with age data:

```
#############################################################
#RIGHT-CENSORED WEIBULL PDF
#age - vector with postmortem shell ages in a death assemblage
#theta - logged model parameters
#lp is r in the Weibull density
#cp is k in the Weibull density
weibull=function(theta, age) {
        logf = function(age, lp, cp) {
        C<-(1/lp)*gamma(1+1/cp)
        lik<-(1/C)*exp(-(lp*age)^cp)
        lik=log(lik)
        age=age
        lp=exp(theta[1])
        cp=exp(theta[2])
        norm=norm
return(-sum(logf(age, lp, cp)))
}

#optim() function can be used for parameter estimation
#start1=c(log(0.0005),log(1))
#optim(par=start1, fn=nweibull, age,  gr=NULL)


#############################################################################
# RIGHT-CENSORED RANDOM-TIME TWO-PHASE EXPONENTIAL PDF
#X - vector with postmortem shell ages in a death assemblage
#out$tau is tau - burial from TAZ to SZ (or stabilization)
#out$lambda1 is lambda 1 - rate of disintegration in TAZ
#out$lambda2 is lambda 2 - rate of disintegration in SZ and/or removal from SZ

FitExpMix=function(X,niters=10000,a=2,b=0.001,rmean=mean(X)){
## prior on beta=Beta(a,a); posterior = Beta(a+N1,a+N2)
## prior on r1 & r2 =Gamma(b,1/(rmean*b); posterior = Gamma(b+n,1/(rmean*b+mean(X1 or
##X2)*n))
N=length(X)
d=function(x){
        r1*exp(-r1*x)*beta+r2*exp(-r2*x)*(1-beta)
        }
        beta=0.5;
        r1=1;
        r2=1;
        best=c(beta,r1,r2);
        dbest=sum(log(d(X)))
        cluster=rbinom(N,1,beta);
```

```
        c=which(cluster==1)
                for(iter in 1:niters){
                        beta=rbeta(1,a+length(c),a+N-length(c))
                        r1=rgamma(1,b+length(c),rate=rmean*b+sum(X[c]));
                        r2=rgamma(1,b+N-length(c),rate=rmean*b+sum(X[-c]))
                        L1=beta*r1*exp(-r1*X)
                        L2=(1-beta)*r2*exp(-r2*X)
                        cluster=rbinom(N,1,L1/(L1+L2));
                        c=which(cluster==1)
                        dnew=sum(log(d(X)));
                        if(dnew>dbest){dbest=dnew;best=c(beta,r1,r2)}
                        }
        beta=best[1];
        r1=best[2];
        r2=best[3]
        if(r1>r2) {beta=1-beta;r1temp=r1;r1=r2;r2=r1temp}
out=list();out$beta=beta;out$r1=r1;out$r2=r2
## convert parameters
out$alpha=(beta*r1)/(beta*r1+(1-beta)*r2)
out$tau=out$alpha*(r2-r1);out$lambda1=r2-out$tau;out$lambda2=r1
out$lik=dbest
out
}

##Approximate computation of completeness, assuming steady-state production since the last
##glacial maximum (~20,000 years).
production=seq(0,20000,by=1)
#one-phase model with estimate of lambda
survived=exp(-lambda*production)
#Weibull model with estimate of r and k
survived=exp(-(r*production)^k)
#2-phase model with estimate of lambda 1, lambda2, tau
#alpha=tau/(lambda1+tau-lambda2)
survived=exp(-lambda2*production)*alpha+exp(-(lambda1+tau)*production)*(1-alpha)
completeness=sum(survived)/max(production)
```

Table DR1 – Coordinates and water depths of 18 sites with *Nuculana taphria* and *Parvilucina tenuisculpta*. Site ID numbers are those of the Bight'03 survey, which is also the source of data on numbers of living individuals. Partitioning sites into four regional single-species assemblages (Santa Barbara Shelf, Palos Verdes Shelf, San Pedro Shelf, and San Diego Shelf) reduces the depth range per assemblage to <20 m (with the exception of *Parvilucina tenuisculpta* from the Palos Verdes Shelf, 44 m depth range).

Site ID	Region	Sediment type	Depth (m)	Year of sampling	Longitude	Latitude	%sand	Grab penetration (cm)	Species	Abundance alive	Number of dated shells
4042	Palos Verdes Shelf	muddy sand	28	2003	-118.296191	33.695483	66.76	14	*N. taphria*	1	20
4170	Palos Verdes Shelf	muddy sand	25	2003	-118.303776	33.698482	78.98	11	*N. taphria*	1	5
4047	San Barbara Shelf	muddy sand	24.7	2003	-119.66209	34.3956	68.86	12.5	*N. taphria*	0	25
4267	San Barbara Shelf	mud	30.6	2003	-119.43346	34.31313	8.41	15	*N. taphria*	6	10
4058	San Pedro Shelf	muddy sand	28	2003	-118.079117	33.642617	76.79	7	*N. taphria*	1	10
4090	San Pedro Shelf	muddy sand	29	2003	-118.130697	33.659615	74.43	12	*N. taphria*	1	10
4122	San Pedro Shelf	muddy sand	48	2003	-118.140479	33.604468	80.24	8	*N. taphria*	1	16
4137	San Pedro Shelf	muddy sand	57	2003	-118.011507	33.576949	82.62	7	*N. taphria*	0	15
4265	San Pedro Shelf	muddy sand	40	2003	-118.026628	33.591817	73.62	8	*N. taphria*	0	25
4290	San Pedro Shelf	sandy mud	23	2003	-118.184554	33.711698	46.51	16	*N. taphria*	5	25
4362	San Pedro Shelf	muddy sand	51	2003	-118.248063	33.637183	70.62	11	*N. taphria*	0	25
4369	San Pedro Shelf	muddy sand	56	2003	-117.984603	33.575269	78.22	8	*N. taphria*	0	10
4036	Sand Diego Shelf	muddy sand	48	2003	-117.305167	32.796183	63.23	12.5	*N. taphria*	1	25
4244	Sand Diego Shelf	sandy mud	57	2003	-117.282	32.682217	49.69	11	*N. taphria*	1	5
4248	Sand Diego Shelf	sandy mud	58	2003	-117.281567	32.679167	49.88	10	*N. taphria*	2	7
4042	Palos Verdes Shelf	muddy sand	28	2003	-118.296191	33.695483	66.76	14	*P. tenuisculpta*	1	6
4070	Palos Verdes Shelf	sandy mud	72	2003	-118.446191	33.758516	39.6	15	*P. tenuisculpta*	0	25
4170	Palos Verdes Shelf	muddy sand	25	2003	-118.303776	33.698482	78.98	11	*P. tenuisculpta*	3	15
4326	Palos Verdes Shelf	muddy sand	41	2003	-118.423747	33.742965	56.13	14	*P. tenuisculpta*	3	26
4119	San Barbara Shelf	muddy sand	18.8	2003	-119.843311	34.400081	89.14	8.5	*P. tenuisculpta*	1	25
4090	San Pedro Shelf	muddy sand	29	2003	-118.130697	33.659615	74.43	12	*P. tenuisculpta*	1	4
4122	San Pedro Shelf	muddy sand	48	2003	-118.140479	33.604468	80.24	8	*P. tenuisculpta*	0	10
4137	San Pedro Shelf	muddy sand	57	2003	-118.011507	33.576949	82.62	7	*P. tenuisculpta*	3	25
4234	San Pedro Shelf	sand	34	2003	-118.264827	33.671651	96.54	7	*P. tenuisculpta*	1	50
4265	San Pedro Shelf	muddy sand	40	2003	-118.026628	33.591817	73.62	8	*P. tenuisculpta*	2	15
4362	San Pedro Shelf	muddy sand	51	2003	-118.248063	33.637183	70.62	11	*P. tenuisculpta*	0	10
4369	San Pedro Shelf	muddy sand	56	2003	-117.984603	33.575269	78.22	8	*P. tenuisculpta*	2	25
4036	Sand Diego Shelf	muddy sand	48	2003	-117.305167	32.796183	63.23	12.5	*P. tenuisculpta*	0	15
4244	Sand Diego Shelf	sandy mud	57	2003	-117.282	32.682217	49.69	11	*P. tenuisculpta*	4	10

Table DR2 – Radiocarbon and amino acid racemization data used to generate AAR calibration curves. Note: sd = standard deviation; Asp = aspartic acid; Glu = glutamic acid.

Specimen code	Species	Collected	Water depth (m)	14C age (yr BP)	Age error (yr)	Calibrated age (years before 2003)	Calibrated age uncertainty (one-half of 2 sigma range)	D/L Asp	D/L Glu	Site ID	NOSAMS accession number
NT4042-13	*Nuculana taphria*	Dead	28	980	30	430	183	0.122	0.040	4042	OS-77178
NT4042-2	*Nuculana taphria*	Dead	28	1000	25	446	171	0.159	0.048	4042	OS-77177
NT4170-2	*Nuculana taphria*	Dead	25	2000	30	1373	218	0.227	0.075	4170	OS-77176
NT4265-8	*Nuculana taphria*	Dead	40	4170	30	3980	281	0.275	0.085	4265	OS-77180
NT41-3	*Nuculana taphria*	Dead	89	13850	75	15701	463	0.330	0.097	41	OS-74071
NT41-4	*Nuculana taphria*	Dead	89	17050	130	19640	339	0.462	0.159	41	OS-74072
NT41-15	*Nuculana taphria*	Dead	89	14950	75	17199	553	0.429	0.138	41	OS-74160
NT41-20	*Nuculana taphria*	Dead	89	2270	45	1659	246	0.241	0.073	41	OS-77191
NT50-14	*Nuculana taphria*	Dead	89	14250	75	16248	480	0.444	0.140	50	OS-74075
NT50-5	*Nuculana taphria*	Dead	89	11250	55	12664	300	0.372	0.110	50	OS-74074
PT4119-1	*Parvilucina tenuisculpta*	Dead	18.8	3440	30	3075	254	0.267	0.082	4119	OS-80898
PT4119-3	*Parvilucina tenuisculpta*	Dead	18.8	2370	35	1773	246	0.208	0.064	4119	OS-80909
PT4362-9	*Parvilucina tenuisculpta*	Dead	51	935	30	394	204	0.100	0.028	4362	OS-80901
PT4119-5	*Parvilucina tenuisculpta*	Dead	18.8	2340	50	1739	260	0.245	0.072	4119	OS-80910
PT4042-2	*Parvilucina tenuisculpta*	Dead	28	805	45	251	200	0.097	0.031	4042	OS-81023
PT4369-15	*Parvilucina tenuisculpta*	Dead	56	9380	45	9966	296	0.305	0.112	4369	OS-80902
NT50-9	*Nuculana taphria*	Dead	89	>Modern	NA	NA	NA	0.069	0.031	50	OS-76150
PT4170-7	*Parvilucina tenuisculpta*	Dead	25	>Modern	NA	NA	NA	0.092	0.039	4170	OS-80440
PT4119-11	*Parvilucina tenuisculpta*	Dead	18.8	>Modern	NA	NA	NA	0.105	0.041	4119	OS-80438
NE41	*Nuculana elenensis*	Live	89	NA	NA	0	NA	0.056	0.020	41	NA
PT4326-26	*Parvilucina tenuisculpta*	Live	41	NA	NA	0	NA	0.062	0.020	4326	NA

Table DR3 – Calibration statistics for the rate of amino acid racemization (AAR) based on paired AAR and ^{14}C analyses of two mollusc species. These define a regression line, where the expected age in calendar years (before AD 2003) corresponds to slope*(D/L)^exponent, with a y-intercept of zero. n = the number of specimens used for calibration, Adj.R2 = the adjusted coefficient of determination showing the fit strength; SE = mean standard error for shell ages younger than 500 years, 500-5,000 years, and older than 5,000 years. Shells < 500 years old have standard error < 20 years, shells 500-5,000 years old have standard error between 108 and 383 years, and shells > 5,000 years old have standard error between 437-1,162 years.

	Amino acid	n	Intercept	Slope	Exponent	Adj. R2	SE (0-500y)	SE (500-5000y)	SE (>5000y)
Parvilucina tenuisculpta	aspartic acid	6	0	919323	4.004	0.910	4	422	1185
Parvilucina tenuisculpta	glutamic acid	6	0	5920942	2.942	0.985	5	105	411
Nuculana taphria	aspartic acid	9	0	331576	3.576	0.980	3	108	430
Nuculana taphria	glutamic acid	9	0	9208343	3.260	0.931	11	197	775

Table DR4 – Estimated parameters of three probability density functions with negative log-likelihoods, the Akaike Information Criterion corrected for small sample size (AICc), ΔAIC, and Akaike weights (the probability that the given model is the best relative to the other models) for single-species assemblages at the regional scale. Given the data, the models with the Akaike weights exceeding 0.8 (in bold) imply that they are four (or more) times more likely than other models.

	P. tenuisculpta -Santa Barbara	*P. tenuisculpta* -Palos Verdes	*P. tenuisculpta* -San Pedro	*P. tenuisculpta* -San Diego	*N. taphria* -Santa Barbara	*N. taphria* -Palos Verdes	*N. taphria* -San Pedro	*N. taphria* -San Diego
1-phase rate	0.0025	0.0088	0.0013	0.0008	0.0007	0.0014	0.0003	0.0012
Weibull rate	80	0.0939	46	36521	192348	0.0013	933962	14158
Weibull shape	0.19	0.46	0.19	0.13	0.12	1.07	0.11	0.14
2-phase rate 1	0.0192	0.0199	0.0222	0.0287	0.0669	0.0014	0.1255	0.1191
2-phase rate 2	0.00058	0.00098	0.00028	0.00021	0.00021	0.0014	0.00021	0.00062
Sequestration rate	0.00014	0.00007	0.00007	0.00007	0.00008	7E-07	0.00042	0.00067
1-phase -LogLik	174.3	407.4	861	202.6	288	189.2	1238.3	278.9
Weibull -LogLik	150.5	384.3	727	164.3	230.1	189.2	1161.9	248.2
2-phase -LogLik	150.8	375.6	689.1	157	208.7	189.2	1088.8	234.8
1-phase AICc	350.9	816.9	1724	407.3	578.2	380.6	2478.6	560
Weibull AICc	305.5	772.7	1458.2	333	464.7	383	2327.9	500.7
2-phase AICc	308.7	757.6	1384.5	321.1	424.2	383.8	2183.8	476.3
1-phase delta AIC	45.4	59.3	339.5	86.2	154	0	294.7	83.7
Weibull delta AIC	0	15.1	73.7	11.9	40.5	2.3	144.1	24.4
2-phase delta AIC	3.2	0	0	0	0	3.1	0	0
1-phase weight	0	0	0	0	0	0.66	0	0
Weibull weight	**0.83**	0	0	0	0	0.2	0	0
2-phase weight	0.17	**1**	**1**	**1**	**1**	0.14	**1**	**1**

Table DR5 – Estimated parameters of three probability density functions with, the Akaike Information Criterion corrected for small sample size (AICc) for single-species assemblages at the site scales, for sites with more than 15 specimens. Although such samples sizes are still small, AIC values support time-varying models, with seven of 17 local assemblages conforming to two-phase model and eight conforming to the Weibull model with k < 0.5 (Table DR5).

| Species	Sample	Sample size	Median age	Age range	1-phase λ	Weibull r	Weibull k	2-phase λ_1	2-phase λ_2	Median time to burial (years)	1-phase AIC	Weibull AIC	2-phase AIC
P. tenuisculpta	PT 4119-19 m	25	43	3839	0.00255	1017.35	0.16	0.0191	0.00057	4847	350.7	**300.5**	307.9
P. tenuisculpta	PT 4170-25 m	15	108	3328	0.00279	0.08	0.38	0.0077	0.00048	12437	208.7	200.5	**200.4**
P. tenuisculpta	PT 4234-34 m	25	36	118	0.02405	0.01	1.75	0.0241	0.02405	43274	238.6	**239.5**	243.4
P. tenuisculpta	PT 4265-40 m	15	114	4394	0.00124	20.83	0.2	0.0146	0.00036	4938	233	214.7	**212.5**
P. tenuisculpta	PT 4326-41 m	25	30	213	0.02329	0.02	1.04	0.0252	0.01496	526	**240.2**	242.5	245
P. tenuisculpta	PT 4036-48 m	15	103	9057	5e-04	26.14	0.18	0.0094	2e-04	5682	260.6	240.2	**232.4**
P. tenuisculpta	PT 4369-56 m	25	28	9282	0.00138	59	0.2	0.0297	1e-04	56303	381.5	294.6	**264.6**
P. tenuisculpta	PT 4137-57 m	25	28	57	0.03734	0.02	6.63	0.0375	0.03748	31372	216.6	**209.4**	221.3
P. tenuisculpta	PT 4070-72 m	25	33	132	0.02301	0.01	1.75	0.023	0.02302	11603	240.8	**240.4**	245.6
N. taphria	NT 4290-23 m	25	2423	10310	0.00034	0.19	0.25	0.0045	0.00027	1240	451.2	446.9	**446.5**
N. taphria	NT 4047-25 m	25	21	11332	0.00052	>10000	0.12	0.0156	0.00021	7267	430.3	366.2	**360.4**
N. taphria	NT 4042-28 m	20	412	2552	0.00154	0	0.99	0.0018	0.00144	619	**301.2**	303.7	306.4
N. taphria	NT 4265-40 m	25	1	3176	0.0028	>10000	0.07	0.0634	5e-04	9712	346.1	**186.8**	239.9
N. taphria	NT 4036-48 m	25	1102	4498	0.00082	24.93	0.18	0.0128	0.00048	790	407.4	394.7	**392.3**
N. taphria	NT 4122-48 m	16	5789	11901	0.00017	0	8.24	2e-04	0.00017	9903491	311.7	**306.4**	317.4
N. taphria	NT 4362-51 m	25	5092	10757	2e-04	0	6.53	0.0012	0.00021	634	477.3	**468.7**	481.4
N. taphria	NT 4137-57 m	15	5666	8268	0.00018	0	>10000	2e-04	0.00018	761173	290.7	**280.5**	296.5
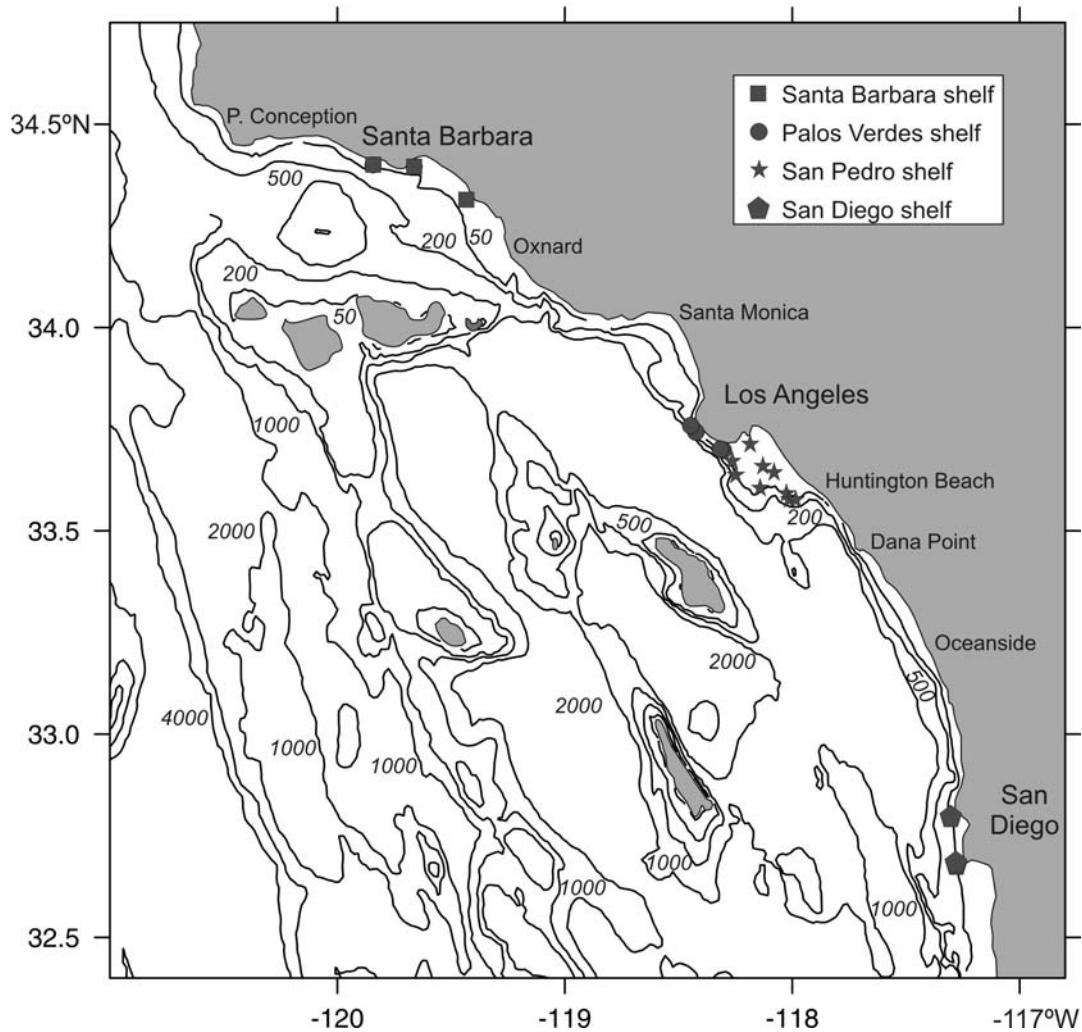
Figure DR1 – Study area and sample sites grouped by shelf segment, Southern California Bight. See Table DR1 for site information including depth range per single-species assemblage. Bathymetric contours in meters. From north to south: Santa Barbara shelf (between Point Conception and Hueneme Canyon), Palos Verdes shelf (between Redondo Canyon and San Pedro Valley), San Pedro shelf (between San Pedro Valley and Newport Canyon), and San Diego shelf (between La Jolla Canyon and US/Mexican border).
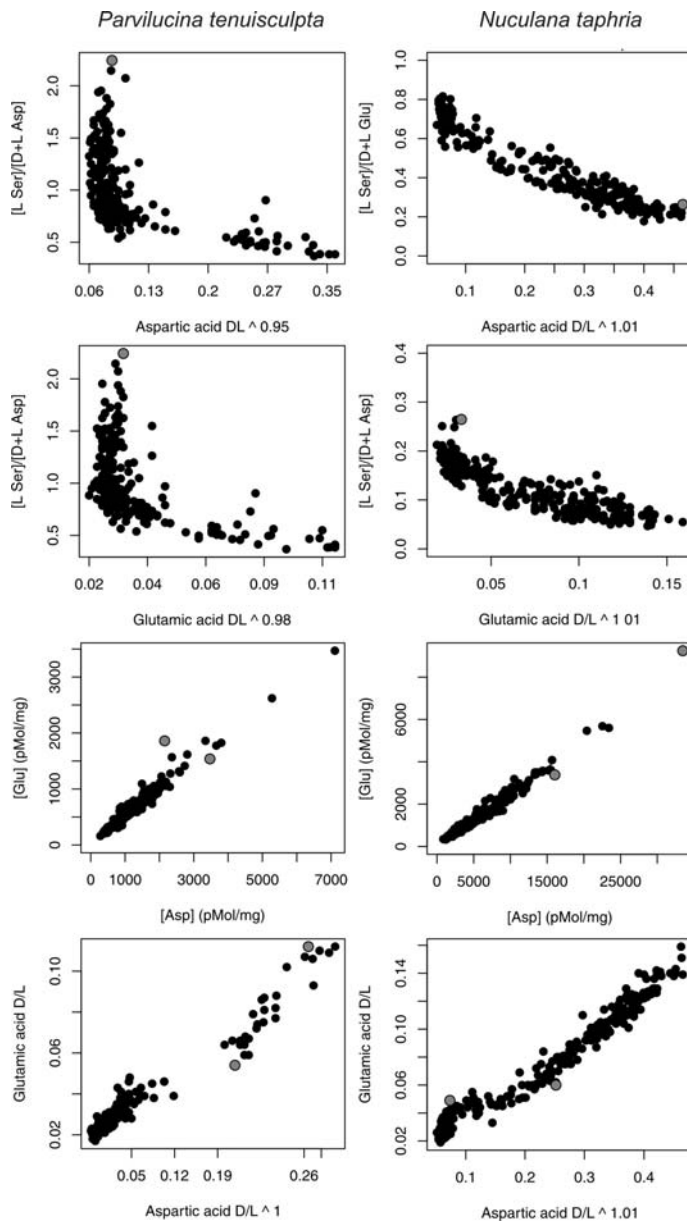
Figure DR2 –Data screening. In the first two rows, L-serine concentrations ([L-Ser]) relative to glutamic acid concentrations ([D+L Glu], upper row) and aspartic acid concentrations ([D+L Asp], second row from top) are plotted against aspartic acid D/L[e] and glutamic acid D/L[e], respectively. The third row shows relationships between concentrations of aspartic acid and glutamic acid. The fourth row shows best-fit exponential relationships between aspartic acid D/L and glutamic acid D/L. Specimens flagged with gray circles are outliers.
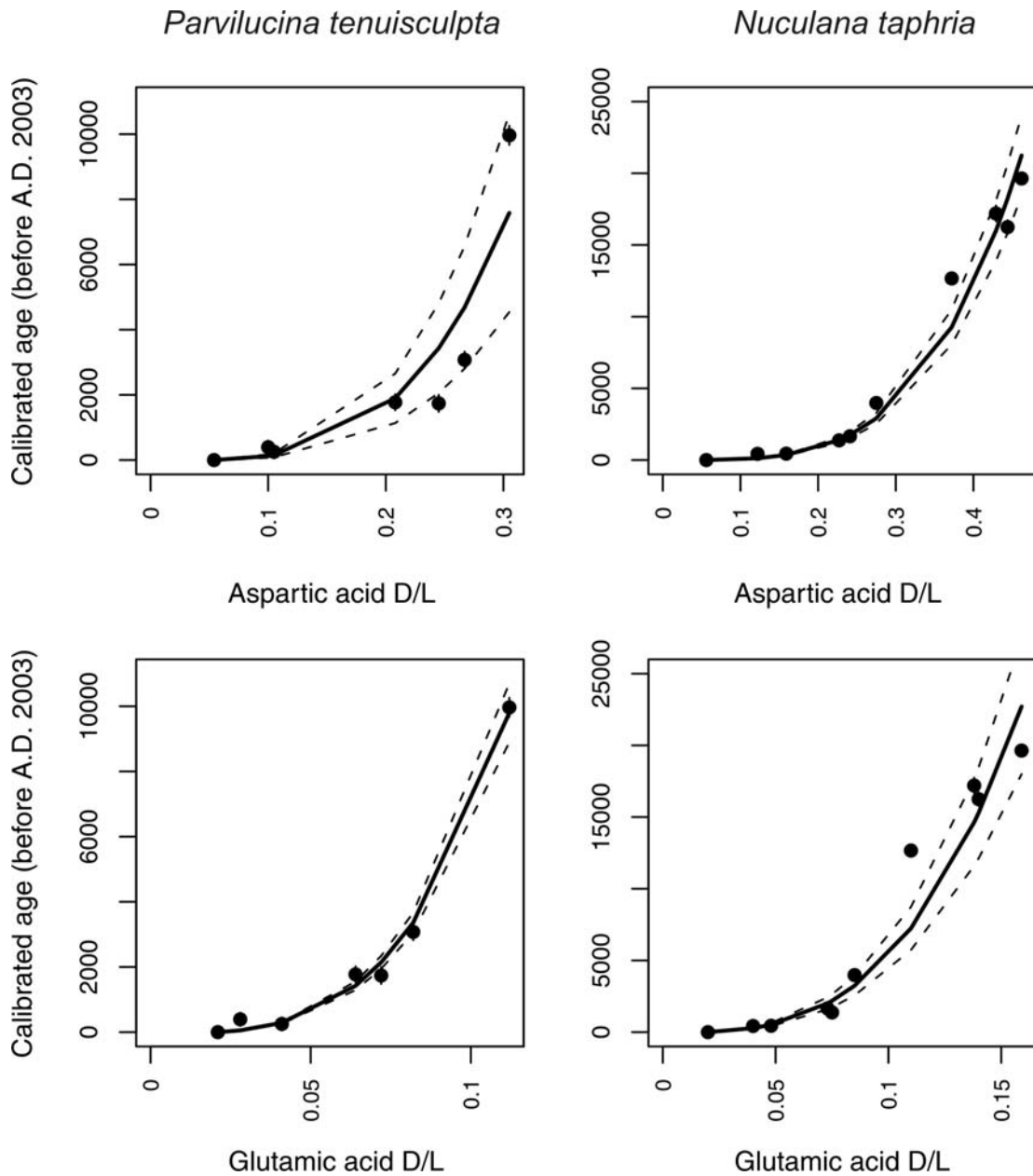
Figure DR3 - Amino acid racemization (AAR) calibration curves for *Parvilucina tenuisculpta* and *Nuculana taphria* shells dated using AMS. Gray dashed lines are 95% prediction intervals. Black vertical line associated with each shell (most are contained within the plot symbol) is the 2σ range of the calibrated age (Calib6.0). Raw data in Table S3.
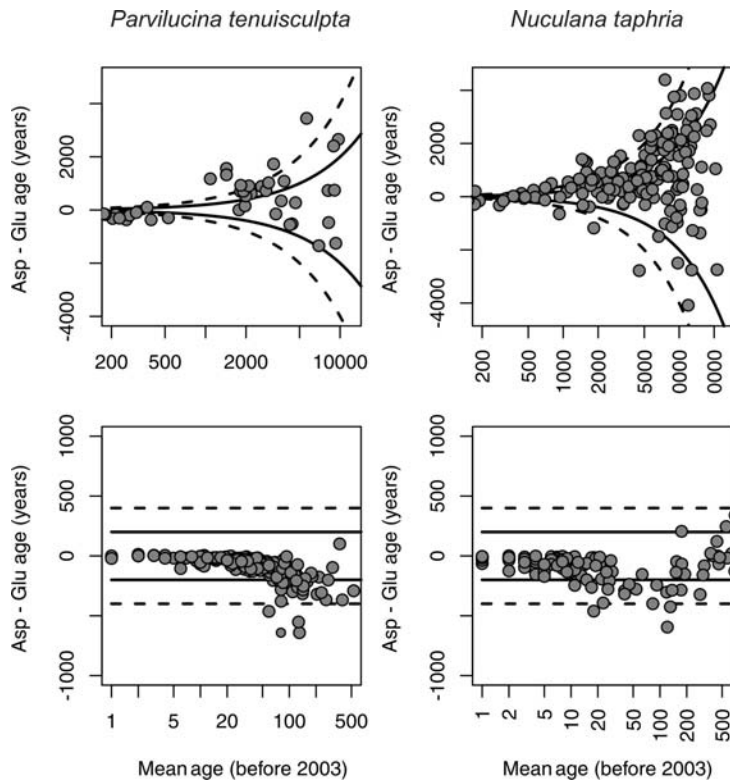
Figure DR4 – Difference in ages inferred from aspartic acid (Asp) and glutamic acid (Glu) is mostly within the range of 20% (solid line) and 40% age uncertainty (dashed line). The upper row shows *proportional* differences between ages relative to the mean age (based on the two age estimates) on the interval between 500 and maximum mean age. The lower row shows *absolute* differences between inferred ages and the mean age on the interval between minimum mean age and 2000 years. Solid lines show differences of 200 years and dashed lines represent differences of 400 years. The mean age uncertainty (averaged across shells) based on the age difference between the aspartic acid and the glutamic acid calibration is 41 years for *Parvilucina* and 59 years for *Nuculana* for shells younger than 1,000 years. The mean proportional age uncertainty is 0.32 for *Parvilucina* and 0.21 for *Nuculana* for shells younger than 1,000 years.
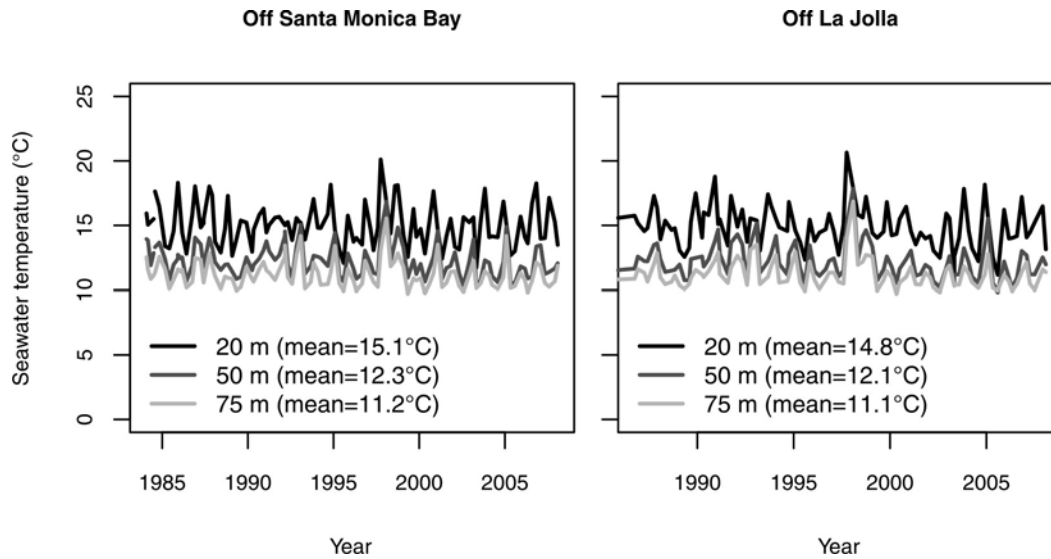
Off Santa Monica Bay   **Off La Jolla**

Figure DR5 - Mean bottom-water temperature today declines by ~3.5-4°C over the depth range of age-dated specimens of *Parvilucina tenuisculpta* (19-72 m) and by ~3°C for *Nuculana taphria* specimens (23-58 m), based on quarterly time series (Ohman and Venrick 2003). Most specimens date from the last 10,000 years; sealevel has risen slowly over this interval by only ~20 m (Nardin et al. 1981) and temperature levels have been stable (Bemis et al. 2002). The small number of older, >10 ka specimens might have been exposed initially to warmer waters at the deepest sampled sites owing to lower sealevel, leading to overestimating their ages relative to those of younger cohorts due to the temperature dependence of racemization rates. However, the entire region was colder during this initial phase of rapid sealevel rise: seawater warmed by several °C up to its present level during the transition from glacial to interglacial 15,000-10,000 years ago (Bemis et al. 2002). Warming rather than cooling has characterized the increase in water depth experienced over the millennial scale of shell accumulation on the southern California shelf, and we thus expect stable temperatures across all sample sites during their windows of time-averaged shell accumulation.
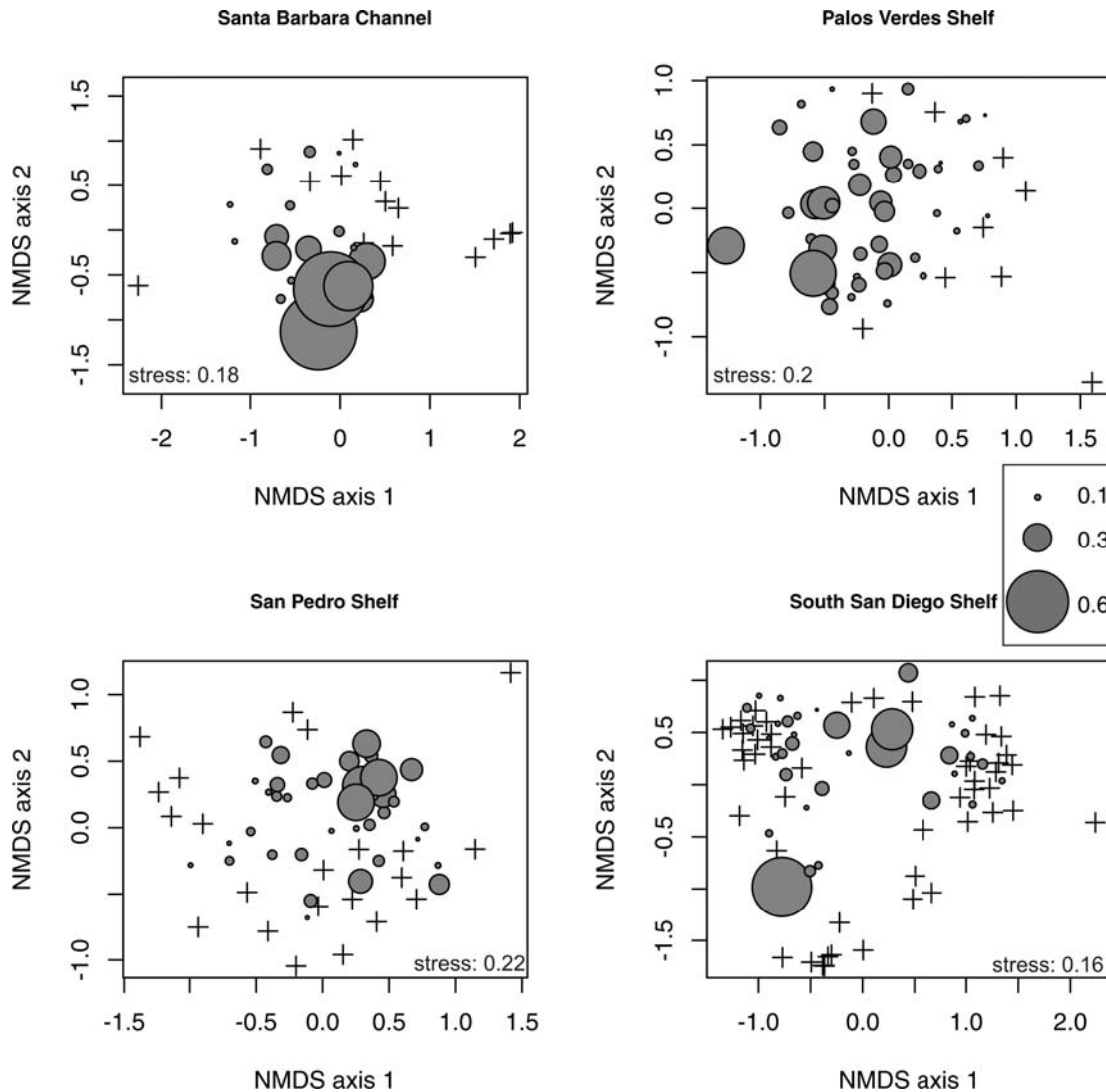
Figure DR6 –Spatial variation among sites in the proportional abundance of living individuals of *Parvilucina tenuisculpta*, showing that this species attained high living abundances in at least some sites in each of the four regions (assemblages sampled between 1990 and 2008; Thompson et al. 1993; Bergen et al. 1998; Ranasinghe et al. 2003, 2007; Stebbins et al. 2004; Ranasinghe et al. 2012). Each point in these non-metric dimensional scaling (NMDS) plots is a living multiple-species assemblage sampled at a different time or site on the seafloor from water depths <75 m between 1997 and 2008; separation of points reflects Bray-Curtis dissimilarities computed using square-root transformed proportional abundances of 150 bivalve species. Gray bubbles denote presence of *P. tenuisculpta*, with bubble diameter indicating its proportional abundance in that living assemblage. Crosses denote living assemblages that did not contain any individuals of *P. tenuisculpta*.
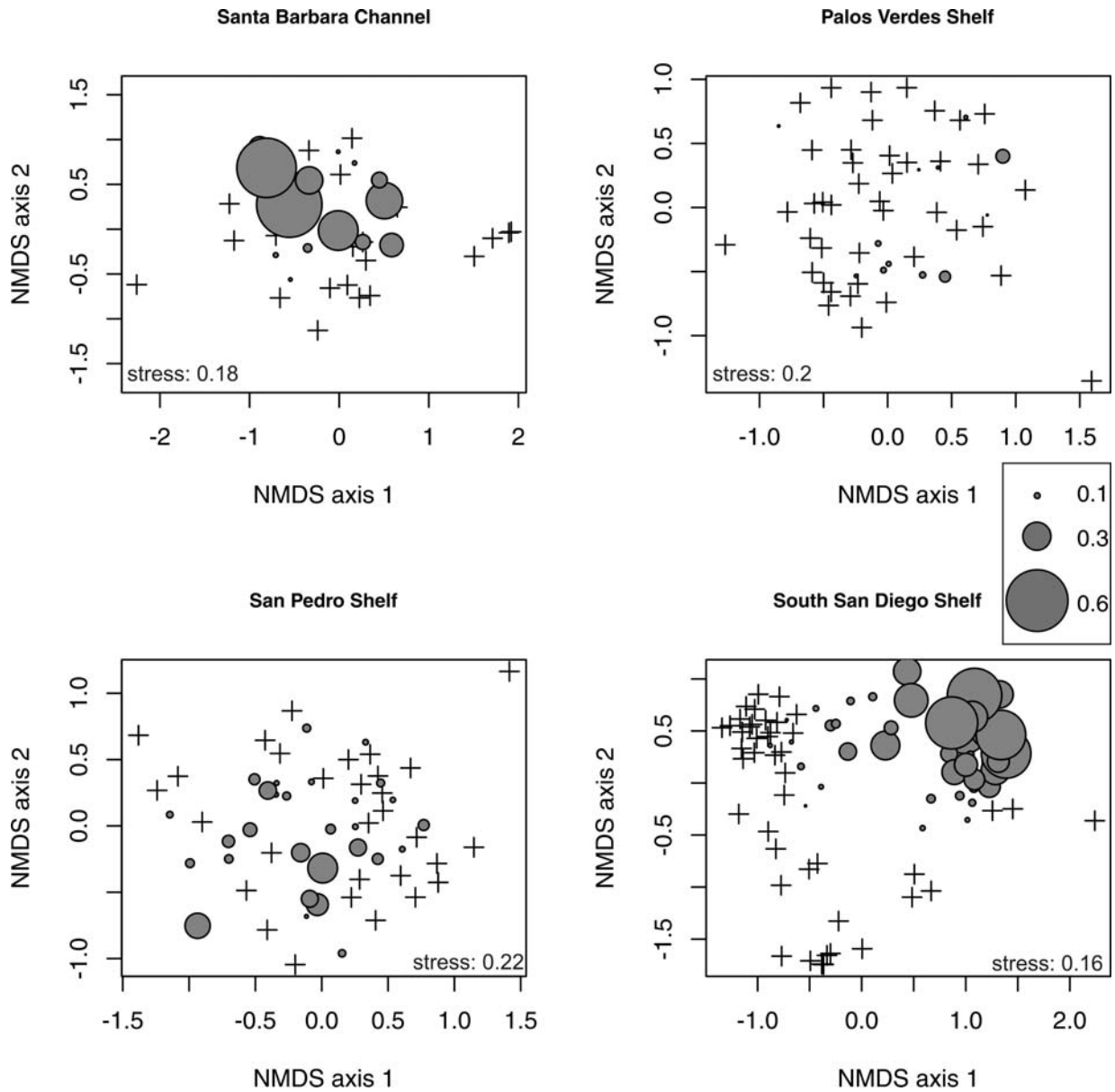
16

Figure DR7 – Counterpart to Figure DR6 showing spatial variation in the proportional abundance of living individuals of *Nuculana taphria.* This species attained moderate to high living abundances at some sites in three regions, but is rare at the Palos Verdes shelf relative to its living abundance in other regions and relative to its abundance in Palos Verdes death assemblages.
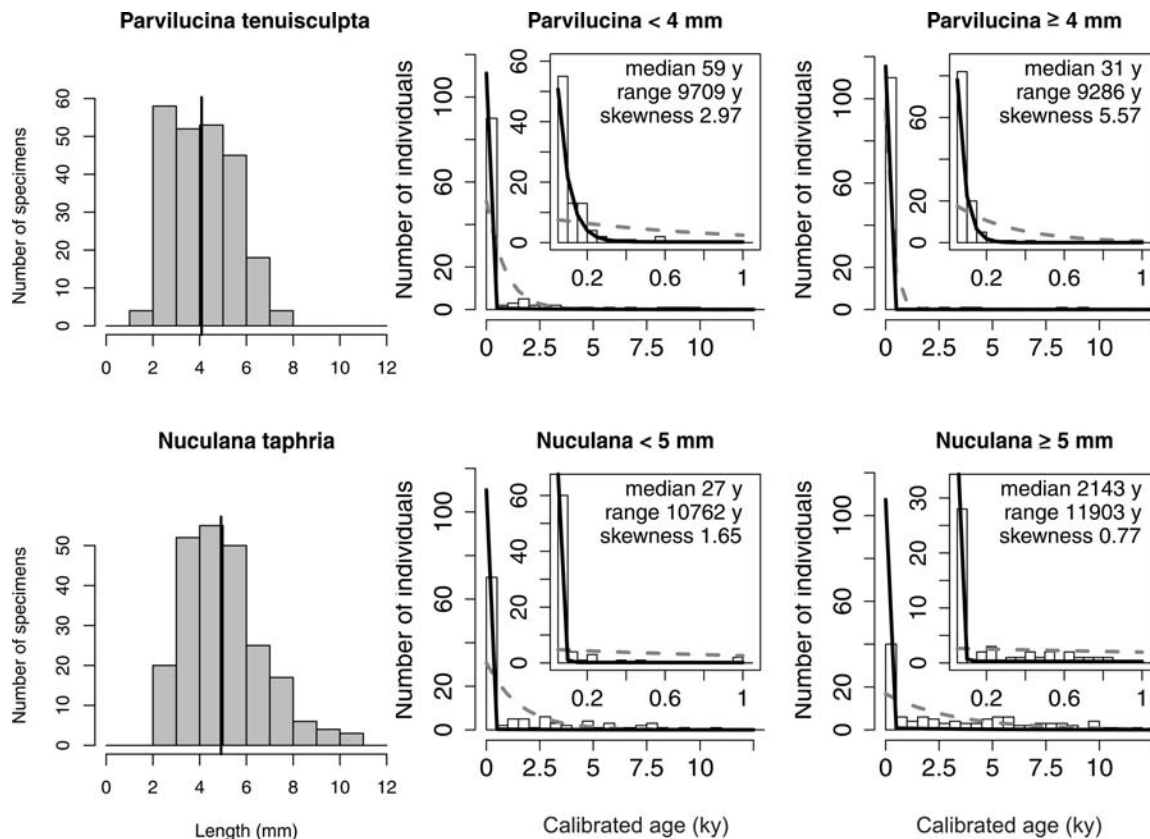
Figure DR8 - Top row: Age-frequency distributions of small (< 4 mm) and large specimens (≥ 4 mm) of *Parvilucina tenuisculpta* have similar medians and age ranges; specimen age and valve length are negatively rank-correlated (rho = -0.26, p < 0.0001), contrary to an expectation that larger shells have higher preservation potential. Bottom row: In contrast, the median age of large (≥ 5 mm) specimens of *Nuculana taphria* is larger than that of small specimens, and specimen age and valve length are significantly positively correlated (rho = 0.38, p < 0.0001). All four AFDs nonetheless show Akaike weights that strongly support the two-phase model (solid black line), indicating that the L-shaped distributions are unrelated to the difference in durability suggested by the *Nuculana* specimens.

Part II. Excel file with raw data on shell ages (Table DR6)

Amino acid racemization data and estimated calendar ages based on radiocarbon calibration. This file will be appended as an excel file, to be briefly embargoed so that we can publish further results on spatial patterns.